Journal of Inflammation Research Dovepress

Open Access Full Text Article ORIGINAL RESEARCH

Mangiferin Ameliorates CCl_4-Triggered Acute Liver Injury by Inhibiting Inflammatory Response and Oxidative Stress: Involving the Nrf2-ARE Pathway

Caixing Shi[1], Yueyao Li[2], Zhidong You[3], Yiran Tian[4], Xiaoyu Zhu[4], Hao Xu[4], Menghan Yang[4], Yutong Zhang[4], Rui Dong[4], Huirong Quan[4], Yongyi Shang[4], Xiaojin Li[1]

[1]School of Basic Medicine, Jining Medical University, Jining, 272067, People's Republic of China; [2]College of Integrated Chinese and Western Medicine, Jining Medical University, Jining, 272067, People's Republic of China; [3]School of Nursing, Jining Medical University, Jining, 272067, People's Republic of China; [4]School of Clinical Medicine, Jining Medical University, Jining, 272067, People's Republic of China

Correspondence: Xiaojin Li, School of Basic Medicine, Jining Medical University, No. 133 hehua Road, Taibai Lake New District, Jining, 272067, People's Republic of China, Tel +8615265775150, Email jinli10221@163.com

Purpose: Acute liver injury (ALI) is characterized by inflammation and oxidative stress (OS). Although mangiferin (MGF) has antioxidant and anti-inflammatory effects, its role in ALI remains unclear. Accordingly, we investigated the MGF molecular mechanism in carbon tetrachloride (CCl_4)-induced ALI in vivo and in vitro.

Materials and Methods: The CCl_4 was utilized to induce ALI in mice. In vivo, the therapeutic effects of MGF on CCl_4-induced liver injury were evaluated through biochemical assays and histomorphological analysis. Additionally, immunohistochemistry, immunofluorescence, ELISA and Western blotting were further applied to explore the mechanism. In vitro, The CCK-8 assay and flow cytometry were employed to investigate the protective effects of MGF against CCl_4-induced toxicity in HepG2 cells, while mitochondrial reactive oxygen species levels and Western blotting were used to explore the biological effects and molecular mechanisms.

Results: MGF treatment resulted in a reduction in serum levels of AST and ALT, diminished concentrations of TNF-α, IL-6, and IL-1β in liver tissue, and concurrently decreased cellular apoptosis. Furthermore, MGF pretreatment enhanced the activity of SOD and GSH while concurrently diminishing the MDA production. This study further demonstrated the upregulation of Nrf2, NQO1, and HO-1 protein expression levels, as well as the downregulation of p-p65 protein expression levels. In vitro investigations revealed that the mitigation of CCl_4-induced inflammation and OS by MGF was mediated via the Nrf2- antioxidant response element (ARE) pathway, which was disrupted by ML385 in HepG2 cells.

Conclusion: CCl_4 can induce liver injury, while treatment with MGF mitigates ALI by inhibiting oxidative stress, inflammation, and apoptosis. The protective mechanism of MGF is mediated by the Nrf2-ARE pathway activation.

Keywords: mangiferin, liver injury, oxidative stress, inflammation, Nrf2

Introduction

The liver is crucial for several physiological functions, including blood volume regulation, nutrient metabolism, lipid and cholesterol homeostasis, immune system support, and detoxification.[1] Consequently, the liver is vulnerable to a multitude of threats. Liver injury encompasses various liver function impairments resulting from various factors, including toxic injury, alcoholism, viral infections, and metabolic disorders.[2,3] Without prompt prevention and treatment, these conditions may progress to more severe forms of liver disease, including hepatitis, cirrhosis, and potentially liver cancer, significantly threatening overall health.[4] Currently, the therapeutic options available for the treatment of acute liver injury

Received: 31 May 2024
Accepted: 27 September 2024
Published: 4 October 2024

in clinical practice are limited, and these medications are associated with specific adverse effects.[5] Consequently, the identification and development of novel agents for the prevention and treatment of ALI are of crucial importance.

Carbon tetrachloride (CCl_4) is a potent hepatotoxin commonly utilized in the creation of experimental animal models to mimic liver injury observed in humans.[6] This allows for assessing the potential hepatoprotective properties of different functional components. The hepatotoxic effects of CCl_4 are primarily caused by the induction of OS and inflammation.[7] In hepatotoxicity, liver cytochrome P450 enzymes convert CCl_4 into free radicals that damage proteins, lipids, and DNA, leading to lipid peroxidation and membrane disruption in liver cells, which is reflected by the elevation of alanine transaminase (ALT) and aspartate transaminase (AST) levels in the blood.[8] Furthermore, free radicals stimulate neutrophils and inflammatory cells to secrete mediators, including tumor necrosis factor (TNF)-α, interleukin (IL)-1β, and IL-6, which further disrupt physiological balance, resulting in metabolic dysregulation, necrosis, and liver damage.[9] Consequently, incorporating dietary components rich in antioxidants and anti-inflammatory properties may offer potential benefits in ameliorating liver damage.

Nuclear factor erythroid 2-related factor 2 (Nrf2) is an essential regulator of antioxidant defense mechanisms and significantly attenuates OS-induced damage.[10] Under basal conditions, Nrf2 is sequestered in the cytoplasm by its inhibitor Keap1.[11] However, the interaction between Nrf2 and Keap1 is disrupted during OS, allowing Nrf2 to translocate into the nucleus. Within the nucleus, Nrf2 acts as a master transcriptional activator, inducing the expression of a wide array of antioxidant genes, including those encoding NAD(P)H quinone dehydrogenase 1 (NQO1) and heme oxygenase-1 (HO-1), which are essential for counteracting oxidative damage.[12] The orchestrated upregulation of antioxidant enzymes mediated by Nrf2 has been extensively documented to significantly mitigate liver injury, highlighting its substantial therapeutic potential for treating liver diseases characterized by OS.[13]

Mangiferin (MGF; Figure 1A) is a naturally occurring compound prevalent in Chinese herbs, including mango (*Mangifera indica*), anemarrhena (*Anemarrhena asphodeloides*), agarwood (*Aquilaria sinensis*), guava (*Psidium guajava*), and many others.[14–16] This compound is noted for its significant antioxidant and anti-inflammatory properties.[17,18] Moreover, MGF may offer therapeutic benefits in treating acute organ injuries, particularly in the lung, kidney, and cardiovascular systems.[19–21] Additionally, MGF exhibits several pharmacological effects, including immunomodulatory, anti-diabetic, anticancer, antibacterial, antiviral, and neuroprotective activities.[22,23] Research has elucidated that oral MGF administration in adults does not have notable adverse effects, indicating a lack of toxicity in humans.[24] Consequently, MGF has become a highly promising candidate for antioxidant therapy.[25] Nevertheless, the precise protective mechanisms of MGF against CCl_4-triggered ALI remain ambiguous. Hence, we aimed to assess the effect of MGF on CCl_4-triggered ALI in mice to ascertain its efficacy in treating ALI and elucidate its mechanisms.

Material and Methods

Chemicals and Reagents

MGF (purity > 98%) was provided by Shanghai Yuanye Biotechnology Co., Ltd. (Shanghai, China), while ALT and AST kits were obtained from the Nanjing Jiancheng Institute of Bioengineering (Nanjing, China). Malondialdehyde (MDA), reduced glutathione (GSH), and superoxide dismutase (SOD) kits were produced by Solarbio Science & Technology Co., Ltd. (Beijing, China). Moreover, hematoxylin and eosin (H&E) were acquired from Shenyang WanLei Technology Co., Ltd. (Shenyang, China). The enzyme-linked immunosorbent assay (ELISA) kits of IL-1β/6 and TNF-α were procured from Shanghai Yamei Bio-Pharmatech Co., Ltd. (Shanghai, China). Antibodies against Nrf2, NQO1, HO-1, Bcl-2, Bax, cleaved Caspase-3, p-p65, and p65 were acquired from ABclonal Technology (Wuhan, China). Antibodies against Lamin B, β-actin and GAPDH were procured from Abcam (Cambridge, UK), and anti-rabbit secondary antibodies were obtained from Proteintech Group Inc. (Wuhan, China). Cell counting kit-8 (CCK-8), mitochondrial superoxide detection, Annexin V-FITC cell apoptosis detection, and ATP detection kits were procured from Biyuntian Biotechnology Co., Ltd. (Shanghai, China).

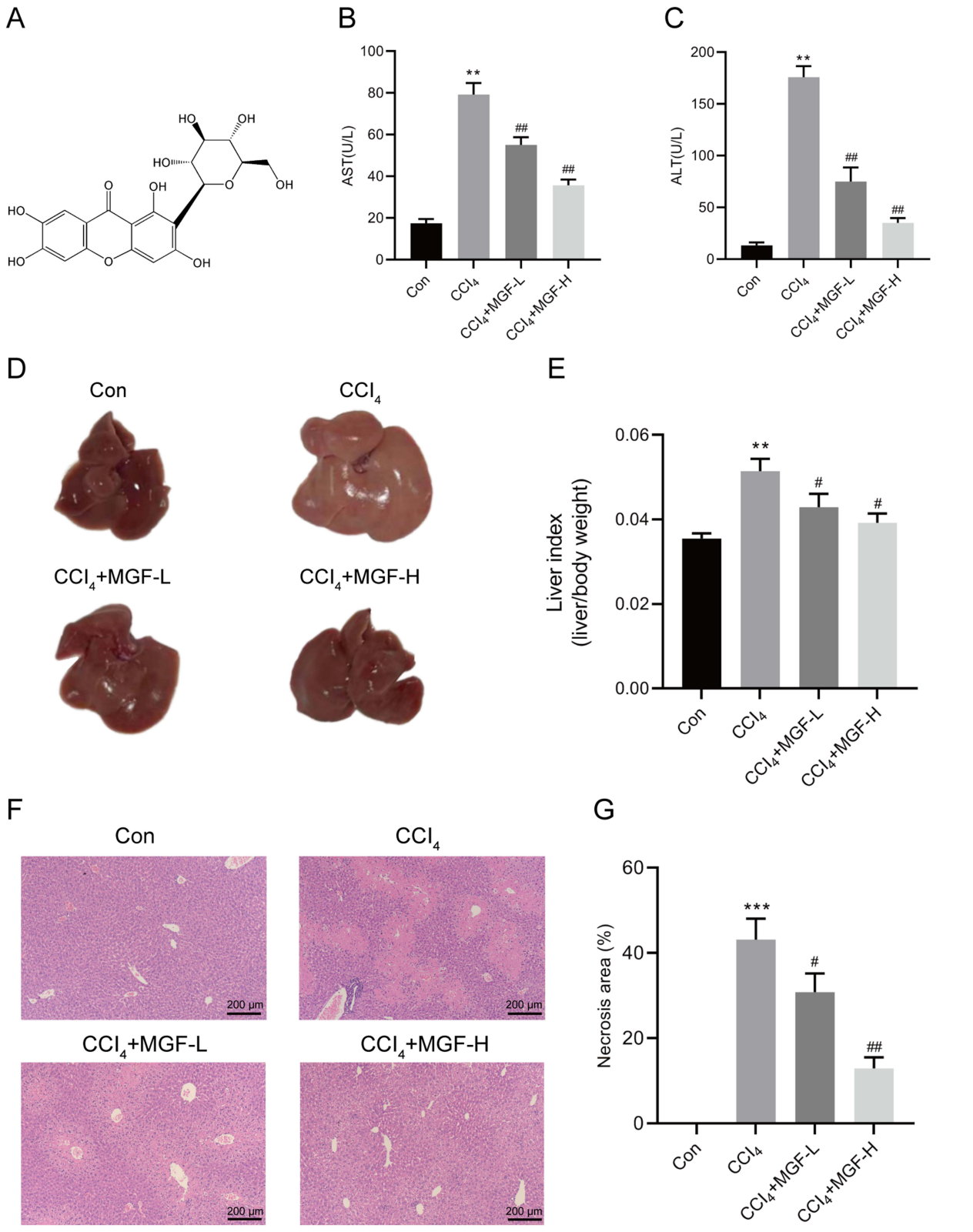

Figure 1 MGF protects against CCl_4-triggered liver injury. (**A**) MGF chemical structure. (**B-C**) AST and ALT levels after the CCl_4 challenge. (**D**) Liver tissue representative image. (**E**) Changes in liver index in the four groups. (**F**) H&E-stained liver section representative image (magnification: 100×), scale bar: 200 μm. (**G**) Quantifying liver tissue necrosis area. Data are expressed as mean ± SD (n = 6). $^{**}P < 0.01$, $^{***}P < 0.001$ versus control group. $^{\#}P < 0.05$, $^{\#\#}P < 0.01$ versus CCl_4 group.

CCl_4-Induced Models and MGF Treatment

Forty adult male ICR mice (eight weeks old; 20–25 g; Jinan Pengyue Experimental Animal Breeding Co., Ltd., Jinan, China) were housed in a 12 h light/dark cycle at 50 ± 5% relative humidity and 21 ± 1 °C, with free access to food and water. All the animal experiments were approved by the Institutional Animal Care and Use Committee of Jining Medical University (JNMC-2023-DW-125). The animals used in this study were handled following the Guide for the Care and Use of Laboratory Animals published by the National Institutes of Health (NIH Publications No. 8023, revised 1978).

The mice were randomly assigned to four groups (n = 10/group): untreated control, CCl_4 model, CCl_4 + low-dose MGF (50 mg/kg), and CCl_4 + high-dose MGF (100 mg/kg). After dissolving CCl_4 in a 1:1 ratio in corn oil, it was intraperitoneally administered to induce ALI at 1.5 mL/kg. The MGF group mice received 50 or 100 mg/kg MGF once daily for a week.

After a week of conditioning, various saline-dissolved MGF doses were administered orally for seven days, with control mice receiving an equivalent volume of saline. After 1 h of the final drug administration, the mice were intraperitoneally injected with CCl_4. Briefly, 24 h later, we collected blood samples from anesthetized mice hearts and centrifuged them at 3000 rpm and 4 °C for 10 min to acquire blood serum stored at –80 °C for additional biochemical analysis. The mice were euthanized, and tissues from the right liver lobe were harvested for subsequent histopathological, immunohistochemical, and immunofluorescence staining analyses. The residual liver tissues were preserved at –80 °C for additional biochemical assays.

Cell Culture and Treatment

HepG2 cells were obtained from the China Cell Line Bank (Beijing, China) and maintained in DMEM supplemented with 10% fetal bovine serum, 100 U/mL penicillin, and 100 U/mL streptomycin at 37 °C in a humidified atmosphere with 5% CO_2. Cells were regularly passaged to maintain logarithmic growth and seeded into appropriate culture plates or flasks. MGF was added at 20 μM for 24 h,[26,27] and the cells were stimulated with 20 mM CCl_4 for 6 h before cell viability was detected.[28] To investigate the role of Nrf2, selected wells were co-treated with 10 μM ML385 (Nrf2 inhibitor) and MGF,[29,30] followed by exposure to 20 mM CCl_4 for 6 h. CCK-8 kits (Biyuntian Biotechnology, China) were used to assess cell viability, and absorbance was measured at 450 nm.

Biochemical Analysis for Liver Markers

ALT and AST levels were quantitatively measured in homogenized liver tissue samples and supernatants from HepG2 cell culture to evaluate the extent of liver injury. Standardized colorimetric assays were employed, following the manufacturer's instructions, to assess enzyme activities indicative of liver damage.

Liver Index Calculation and Histological Examination of Liver Tissues

At the end of the experimental period, each mouse was weighed, and their livers were removed and weighed. The liver index was then calculated using the formula: liver index = (liver weight / body weight) × 100%. Liver tissues were fixed in 4% paraformaldehyde for over 24 h, embedded in paraffin, sectioned (4–5 μm), and stained with H&E. Subsequently, we examined histopathological alterations in the liver using a light microscope and quantified the extent of necrosis using ImageJ (NIH, Bethesda, MD, USA).

TUNEL Assay

Following the dewaxing of liver paraffin-embedded sections, they were incubated with the TUNEL reaction mixture per the instructions, subsequently counterstaining the nuclei with DAPI. The sealed slides were examined using a fluorescence microscope, photographed, and recorded. Six randomly chosen fields were analyzed using the ImageJ software to determine the positive cell number/field.

Liver OS Marker Analysis

Liver tissues and HepG2 cells were collected and homogenized, and the supernatant was collected by centrifugation at 12,000 rpm for 15 min at 4 °C. Using commercially available kits, we quantified the MDA, GSH, and SOD levels per protocol.

TNF-α and IL-1β/6 Level Quantification

Liver tissue homogenates and HepG2 cell culture medium were collected and centrifuged at 12,000 rpm for 15 min at 4 °C to isolate supernatants. TNF-α and IL-1β/6 level quantification in the supernatants were conducted through mouse-specific ELISA kits following the protocols.

Immunohistochemical and Immunofluorescence Staining

Liver tissues were embedded in paraffin, and 5-μm-thick sections were prepared. Following dewaxing and hydration, sections were incubated for 20 min in 0.3% hydrogen peroxide in methanol to suppress endogenous peroxidase activity. The sections were subjected to antigen retrieval by treatment with citrate buffer (pH 6.0) and three rounds of microwave heating for 5 min. After 30 min at room temperature (RT), the sections were blocked using 5% bovine serum albumin (BSA), treated with Bcl-2 and Bax primary antibodies, and incubated at 4 °C overnight. Tissue slices were rinsed three times with phosphate-buffered saline (PBS) and incubated for 1 h with the appropriate horseradish peroxidase (HRP)-conjugated secondary antibody at 37 °C. Following three additional PBS washes, the substrate 3,3'-diaminobenzidine was applied for visualization. Finally, samples were examined and imaged under a microscope.

For immunofluorescence analysis, liver-frozen tissue samples were embedded in OCT compounds to prepare 10-μm-thick frozen sections. These sections were fixed in 4% paraformaldehyde for 30 min, followed by being treated with 3% BSA for 30 min at RT, and incubated overnight with primary antibodies at 4 °C. Subsequently, the slides were exposed to fluorochrome-conjugated secondary antibodies and examined using a fluorescence microscope, and ImageJ software was used to quantify fluorescence intensity.

Western Blotting Analysis

Total and nuclear protein extraction from liver tissues and HepG2 cells was conducted using the Total and Nuclear and Cytoplasmic Protein Extraction Kit (Wanlei Biotechnology, China) according to the manufacturer's protocols, and the protein extracts were quantified using the BCA method. Equal protein concentrations were subjected to electrophoresis on a 10% SDS-PAGE polyacrylamide gel. Afterward, the samples were transferred to a PVDF membrane at low temperatures, rinsed with a blocking solution, blocked for 60 min, and incubated at 4 °C with a primary antibody overnight. Following three washes in TBST the next day, the membrane was incubated for 2 h with an HRP-conjugated secondary antibody at RT. Immunoblots were visualized using an enhanced chemiluminescent substrate (Biyuntian Biotechnology, China) and quantified using ImageJ software (NIH, USA).

Flow Cytometry Analysis

HepG2 cell apoptosis was assessed using annexin V/propidium iodide (PI) double staining and flow cytometry. Following treatment with MGF and CCl_4, the cells were harvested, washed with PBS, and resuspended in a binding buffer. Subsequently, the cells were stained with annexin V-FITC and PI following the manufacturer's instructions (Biyuntian Biotechnology, China). The samples were analyzed by flow cytometry (Beckman Coulter), and the resulting data were analyzed by Kaluza software (Beckman Coulter).

Determination of Mitochondrial Reactive Oxygen Species (ROS)

HepG2 cells were treated for 24 h to quantify mitochondrial ROS according to the specified protocol. After treatment, cells were incubated with MitoSOX Red and MitoTracker Green reagents at 37 °C for 15 min. Subsequently, the cells were washed with PBS to remove the excess probe. Fluorescence microscopy (Nikon, Tokyo, Japan) was used to analyze

the cells. The intensity of MitoSOX Red fluorescence was directly correlated with the level of mitochondrial ROS production.

Determination of ATP content

ATP levels in HepG2 cells were measured using a firefly luciferase-based ATP Assay Kit (Biyuntian Biotechnology, China) following the manufacturer's protocol. The cells were rinsed with PBS, lysed in ATP assay buffer, and ultrasonicated. The supernatant was collected by centrifugation, and 100 μL of it was mixed with 100 μL of ATP detection solution. The luminescence was measured using a microplate reader (Bio-Rad Laboratories, Hercules, CA). ATP concentrations were determined using an ATP standard curve, and protein levels were measured using a BCA protein assay kit. Cellular ATP levels were expressed as nmol/mg of protein.

Statistical Analysis

GraphPad Prism software (version 9; GraphPad Software, San Diego, USA) was used for statistical analysis. Data are reported as the mean ± standard deviation (SD), and their normality was assessed using the Shapiro–Wilk test. Student's *t*-test was employed for normally distributed data to compare continuous variables between the two groups, while the Mann–Whitney *U*-test was used for non-normally distributed data. For multiple comparisons involving more than two groups, we conducted a one-way analysis of variance followed by the Bonferroni post-hoc test for normally distributed data and the Kruskal–Wallis test for non-normally distributed data, with $P < 0.05$ considering statistical significance.

Results

Impact of MGF on CCl_4-Induced ALI in Mice

To assess the therapeutic potential of MGF in mitigating CCl_4-induced ALI, we evaluated its effects on key biochemical markers and histological alterations in mice models. Serum AST and ALT levels increased in the CCl_4-challenged group compared to those in the control group (Figure 1B-C). Compared to the model group, MGF treatment effectively lowered AST and ALT levels in a dose-dependent manner. The liver index was significantly increased in the model group, which was partially reversed by MGF (Figure 1D-E). To further evaluate the protective effect of MGF on CCl_4-induced ALI, we examined liver histopathology. The control group exhibited a fully intact hepatocyte structure with a clear, apparent central vein, whereas the hepatic sinusoids were organized in a radial pattern along the central veins (Figure 1F-G).

Meanwhile, the model group depicted destructed hepatic lobule structure, hyperemia, inflammatory infiltration, and necrosis among the liver lobules. MGF could regenerate liver tissue and effectively decrease the necrotic region compared to the model group. Additionally, it significantly alleviated inflammatory infiltration and liver damage. Accordingly, MGF exerted a protective effect against CCl_4-induced ALI in mice.

Effect of MGF on Hepatocyte Apoptosis in CCl_4-Triggered ALI Mice

TUNEL and IHC assays were conducted to evaluate the effects of MGF on hepatocyte apoptosis in CCl_4-induced ALI mice. Figure 2A-B represent a significantly elevated apoptotic cell percentage (positive for TUNEL staining) in the model group in contrast to the control group, which was dose-dependently diminished by MGF. The IHC assay demonstrated elevated levels of Bax and cleaved Caspase-3, reduced levels of Bcl-2, and a lower Bcl-2/Bax ratio in the model group compared to the control group. These alterations were reversed in the MGF treatment groups relative to the model group (Figure 2C–G). These results suggest that MGF can mitigate hepatocyte apoptosis, exerting a protective effect.

MGF Ameliorated OS and Inflammation in the Mice's Liver Tissues

The hepatic OS biomarkers SOD and GSH were significantly lower, whereas MDA levels were significantly higher in the model group liver tissue than in the control group. MGF treatment significantly reversed these changes compared with the model group (Figure 3A–C). ELISA findings indicated that TNF-α and IL-6/1β levels were significantly higher in the

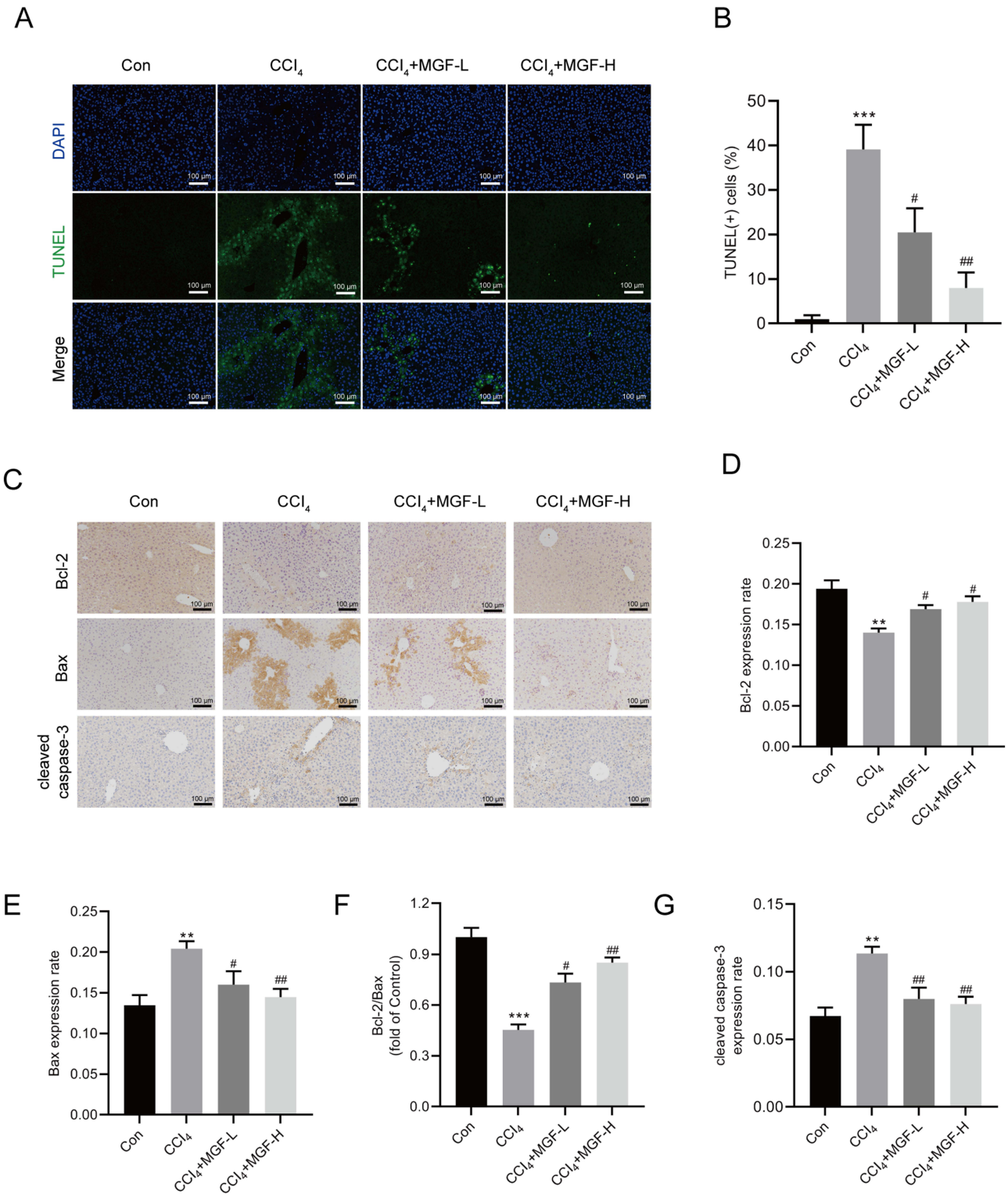

Figure 2 MGF effect on CCl_4-triggered cell apoptosis in liver tissues. (**A**) Representative TUNEL-stained sections demonstrating apoptosis in mice liver tissue (magnification: 200×). (**B**) Statistical analysis of TUNEL-positive cells was performed. (**C**) Determination of Bcl-2, Bax, and cleaved Caspase-3 expression in the liver by immunohistochemistry (original magnification, 200×). (**D–G**) Bcl-2, Bax, Bcl-2/Bax ratio, and cleaved Caspase-3 densitometric analysis. Data are expressed as mean ± SD (n = 6). $^{**}P < 0.01$, $^{***}P < 0.001$ versus control group. $^{\#}P < 0.05$, $^{\#\#}P < 0.01$ versus CCl_4 group.

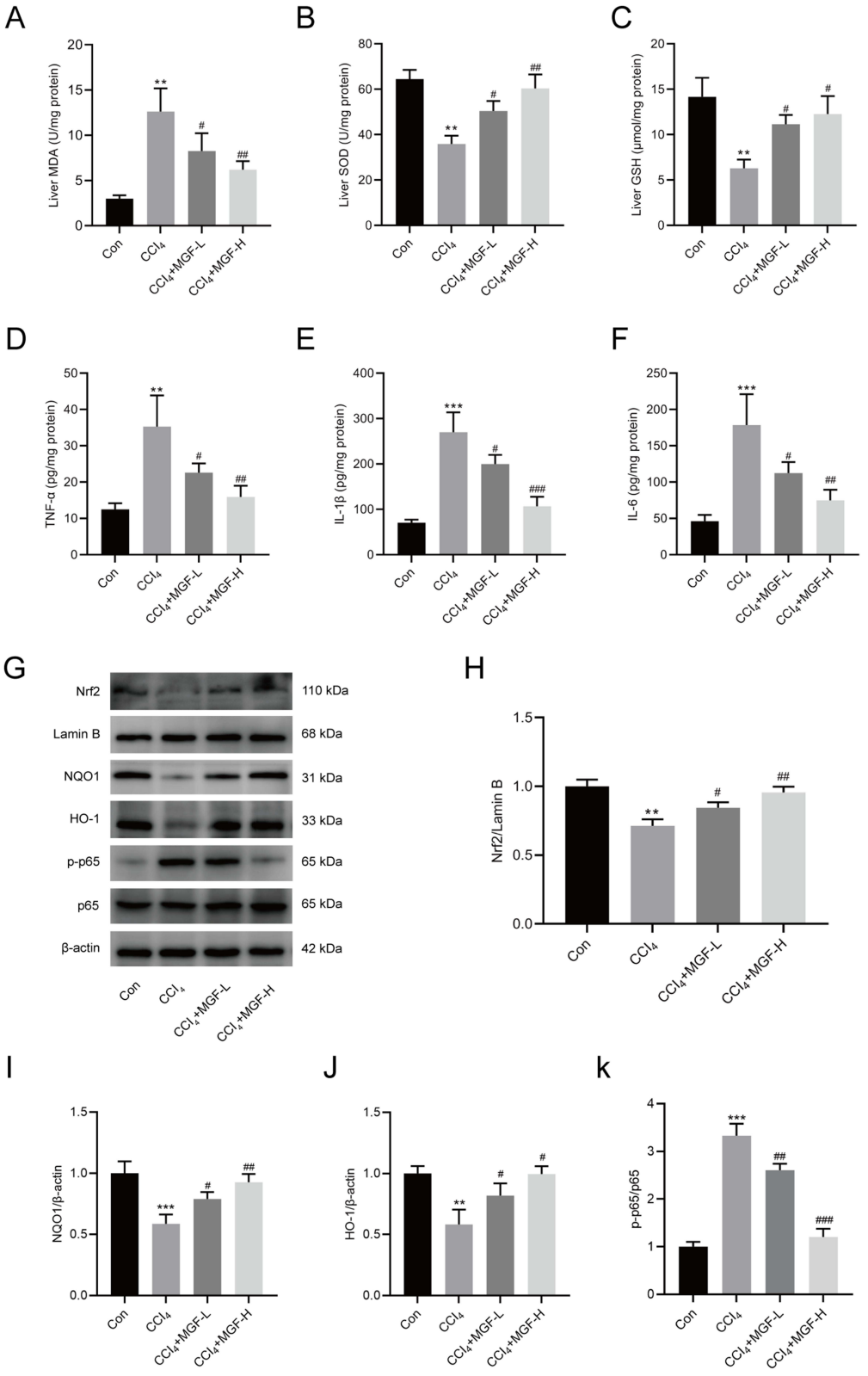

Figure 3 MGF ameliorates CCl_4 exposure-caused OS and inflammatory responses in the mice liver tissues. (**A**) MDA levels (**B**) SOD and (**C**) GSH activities in the mice liver tissues. (**D**) TNF-α, (**E**) IL-1β, and (**F**) IL-6 levels in mice liver tissues. (**G**) Indicating Nrf2, NQO1, HO-1, p-p65 and p65 protein expression in different groups through Western blotting. (**H–K**) Quantification of the Western blotting data for Nrf2, NQO1, HO-1, and p-p65/p65. Data are expressed as mean ± SD (n = 6). $^{**}P < 0.01$, $^{***}P < 0.001$ versus control group. $^{\#}P < 0.05$, $^{\#\#}P < 0.01$, $^{\#\#\#}P < 0.001$ versus CCl_4 group.

model group, while MGF treatment inhibited the expression of proinflammatory factors (Figure 3D–F). These findings suggest that the hepatoprotective effect of MGF is associated with a reduction in OS and inflammatory responses.

MGF Effect on Nrf2-ARE Signaling Pathway in Mice

The Nrf2-antioxidant response element (ARE) pathway is crucial for cellular defense against OS, as it regulates the increase in antioxidant enzymes and protective proteins to combat ROS. Our experimental data, illustrated in Figure 3G–K and Figure 4A–F, revealed through Western blotting and immunofluorescence assays that liver tissues from the model group exhibited a marked reduction in the expression of Nrf2, NQO1, and HO-1, concomitant with a substantial elevation in p-p65 expression. Conversely, The administration of MGF reversed these changes, increasing Nrf2, NQO1, and HO-1 levels while decreasing p-p65 expression. These findings indicate that MGF confers a protective effect by activating the Nrf2-ARE signaling pathway.

MGF Attenuated CCl_4-Induced Cytotoxicity and Apoptosis in HepG2 Cells

To elucidate the impact of MGF on CCl_4-induced cell viability, we conducted a CCK-8 assay. These findings indicated that CCl_4 (20 mM) induced substantial cytotoxicity, which was mitigated by pretreatment with MGF (20 μM) (Figure 5A). However, cell viability was significantly decreased following incubation with ML385. As depicted in Figures 5B–C, ALT and AST levels were reduced after MGF treatment, whereas these levels increased following ML385 treatment. Correspondingly, the cell apoptosis rate was markedly reduced by MGF treatment but was significantly elevated after incubation with ML385 (Figures 5D–J). These findings demonstrate that MGF mediates its hepatoprotective effects through a mechanism dependent on Nrf2.

MGF ameliorated inflammation and OS in HepG2 cells via the Nrf2-ARE pathway

As illustrated in Figures 6A–C, TNF-α and IL-6/1β levels were elevated following CCl_4 treatment. Conversely, these cytokine levels were markedly reduced after MGF treatment. Consistent with our expectations, Nrf2 inhibition increased TNF-α and IL-6/1β expression. Furthermore, MGF pretreatment mitigated CCl_4-induced upregulation of MDA and reduction in SOD and GSH levels. Conversely, inhibition of Nrf2 signaling was associated with decreased SOD and GSH levels, along with an increase in MDA levels, as depicted in Figures 6D–F. Our findings indicate that MGF pretreatment mitigates ROS generation induced by CCl_4 and enhances ATP levels. Conversely, the disruption of Nrf2 signaling results in increased ROS generation and decreased ATP levels (Figures 6G–I). Further studies found that MGF promoted the nuclear translocation of Nrf2, increased the expression levels of NQO1 and HO-1, and inhibited the expression of p-p65. Conversely, administration of ML385 resulted in a reduction in Nrf2 nuclear translocation and the expression of NQO1 and HO-1, while concurrently elevating the expression of p-p65 (Figures 7A–F). These results substantiate our hypothesis that MGF activates Nrf2, attenuating oxidative damage and inflammation.

Discussion

Liver diseases are a major global health issue and cause high annual mortality.[31] Current liver-protection drugs often have limited effectiveness and many side effects, underscoring the urgent need for new, safer hepatoprotective agents.[32] Traditional Chinese medicine has a long history of treating liver disorders, and MGF, a compound from various herbs, demonstrates great promise.[33] Our research suggests that MGF effectively improves liver injury by restoring liver structure and function and reducing inflammation, OS, and apoptosis, highlighting its potential as an innovative therapeutic agent.

The organ index, a vital biological marker for evaluating the functional status of animals, provides concrete evidence of histopathological changes. Previous studies have reported increased liver indices in mice subjected to acute hepatic injury, corresponding to heightened pathological damage.[34] Notably, our research demonstrated that MGF significantly reduced the liver index of CCl_4-induced mice, indicating its therapeutic potential. To corroborate these findings on hepatic tissue morphology, H&E staining of liver sections was performed, which revealed that MGF mitigated hepatocyte necrosis. Blood biochemistry provides a comprehensive assessment of hepatic function in the context of liver diseases.[35] Elevated serum levels of ALT and AST, well-established biomarkers of liver dysfunction, were observed in our study,

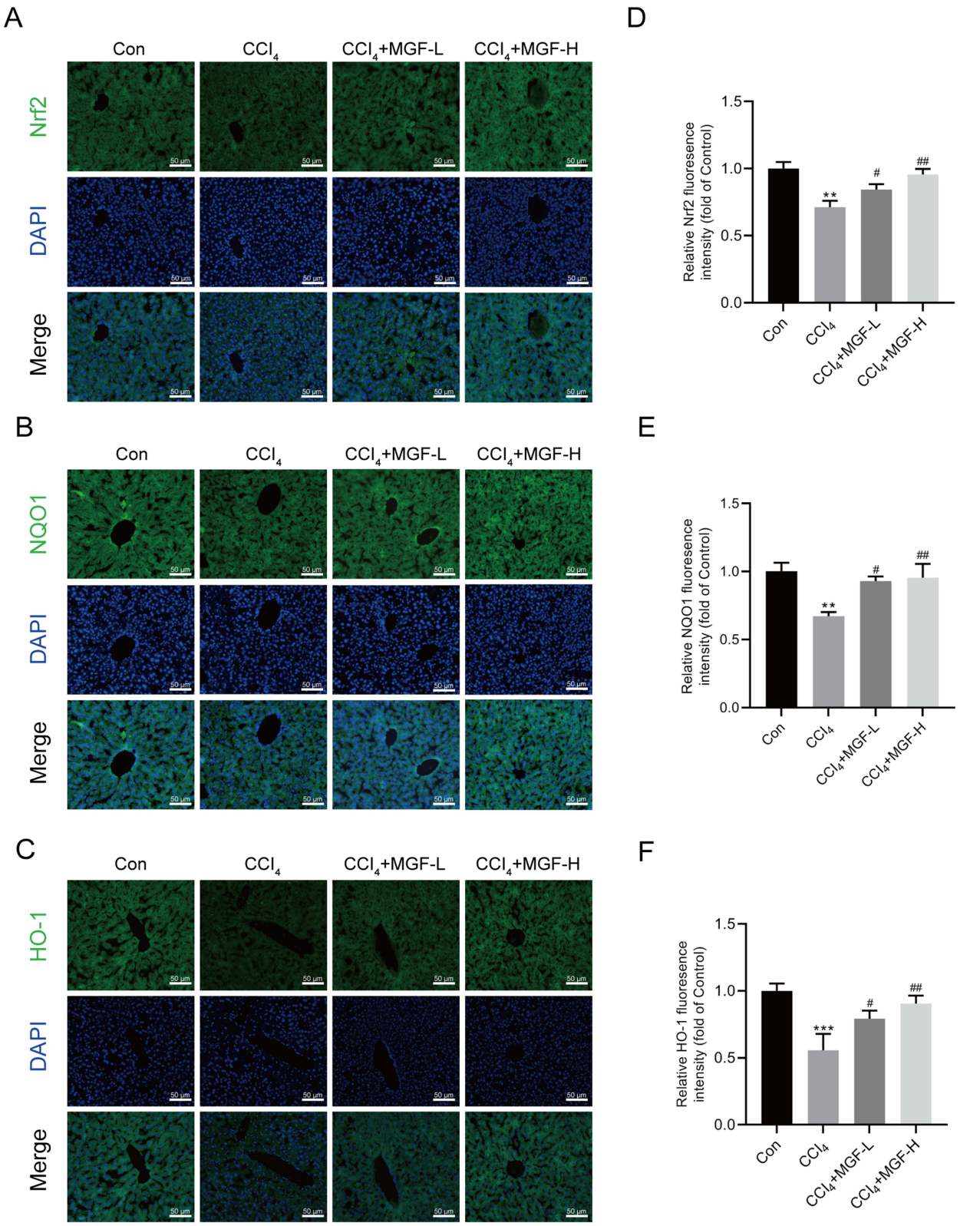

Figure 4 MGF impact on the Nrf2 pathway in CCl_4-treated mice. Immunofluorescence of (**A**) Nrf2, (**B**) NQO1, and (**C**) HO-1 in liver tissues. (**D–F**) Mean integrated optical density of immunofluorescence staining for Nrf2, NQO1, and HO-1. Data are expressed as mean ± SD (n = 6). $^{**}P < 0.01$, $^{***}P < 0.001$ versus control group. $^{\#}P < 0.05$, $^{\#\#}P < 0.01$ versus CCl_4 group.

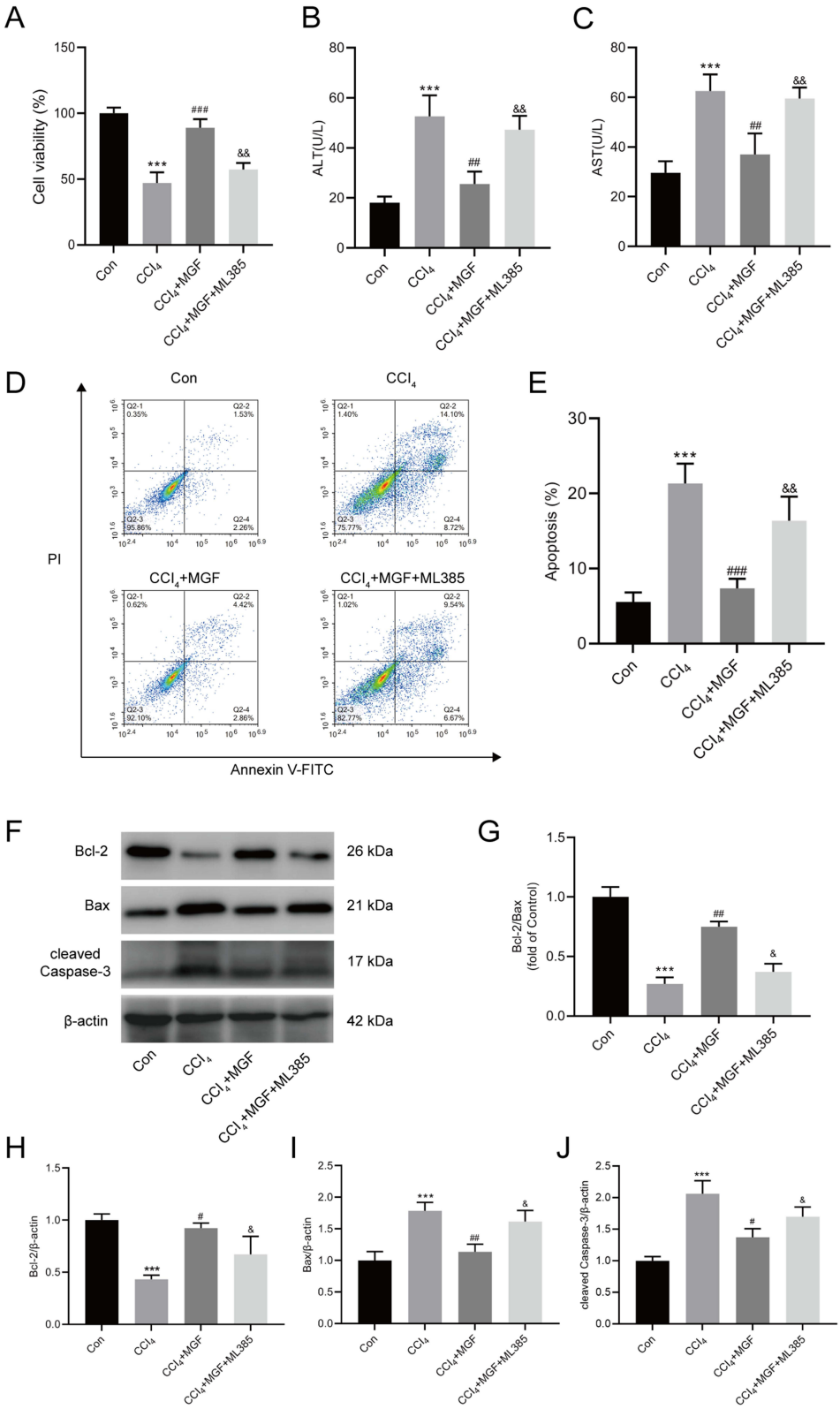

Figure 5 Effect of MGF on CCl_4-induced cytotoxicity and apoptosis in HepG2 cells. (**A**) Cell viability was evaluated using the CCK-8 assay. (**B**) ALT and (**C**) AST levels in the supernatants of HepG2 cells. (**D**) Flow plots of apoptosis in the different groups. (**E**) Quantification of apoptotic cells. (**F**) Indicating Bcl-2, Bax, and cleaved Caspase-3 protein expression in different groups through Western blotting. (**G–J**) Quantitative results for Bcl-2, Bax, Bcl-2/Bax ratio, and cleaved Caspase-3. Data are expressed as mean ± SD (n = 6). $^{***}P < 0.001$ versus control group. $^{\#}P < 0.05$, $^{\#\#}P < 0.01$, $^{\#\#\#}P < 0.001$ versus CCl_4 group. $^{\&}P < 0.05$, $^{\&\&}P < 0.01$ versus CCl_4+MGF group.

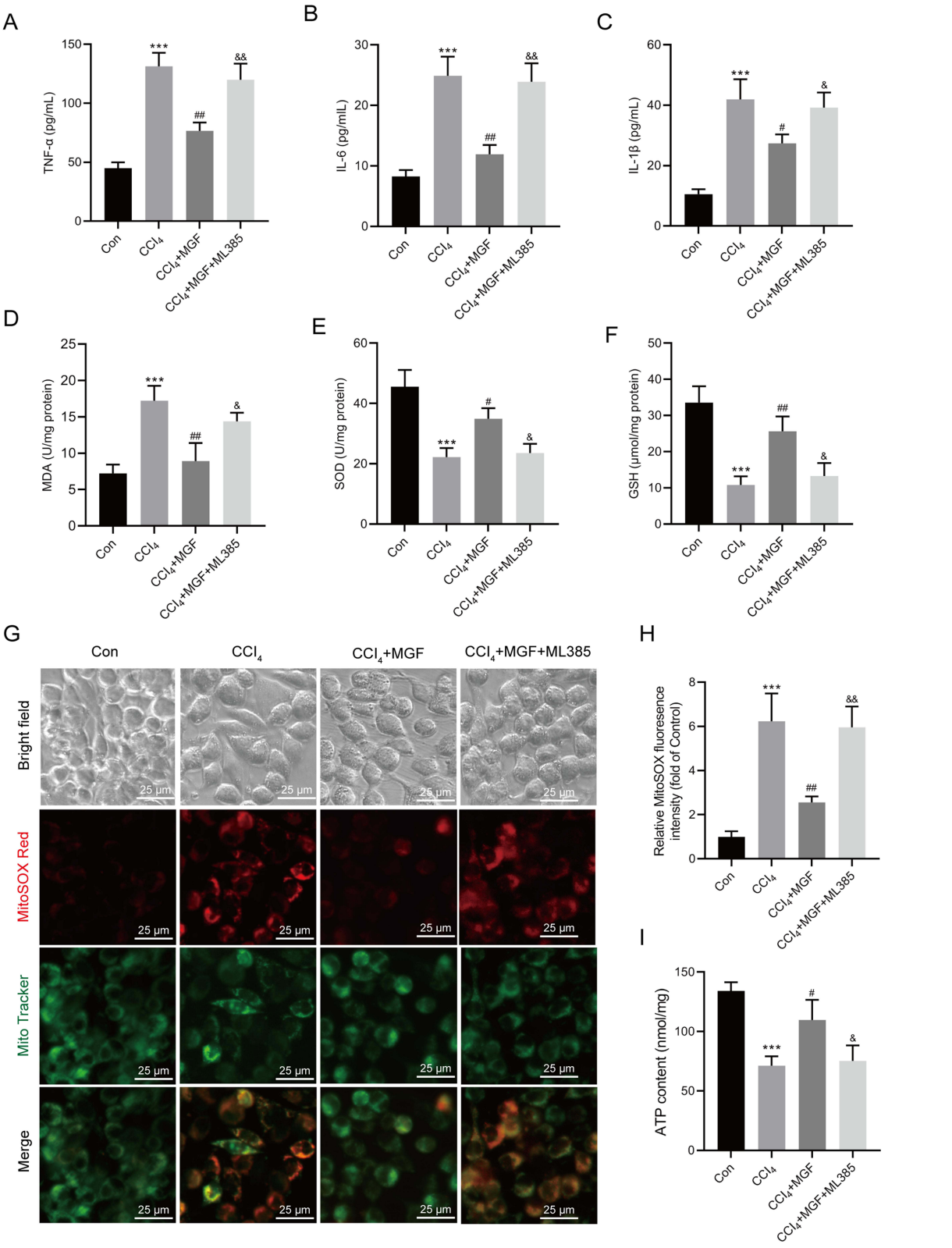

Figure 6 MGF relieves CCl_4-induced inflammatory response and OS in HepG2 cells. (**A**) TNF-α, (**B**) IL-6, and (**C**) IL-1β levels in different groups. (**D**) MDA level, (**E**) SOD, and (**F**) GSH activities in each group. (**G-H**) Mitochondrial superoxide was detected through immunofluorescence using MitoSox Red and MitoTracker Green staining. (**I**) ATP content in different groups. Data are expressed as mean ± SD (n = 6). $^{***}P < 0.001$ versus the control group. $^{\#}P < 0.05$, $^{\#\#}P < 0.01$ versus CCl_4 group. $^{\&}P < 0.05$, $^{\&\&}P < 0.01$ versus CCl_4+MGF group.

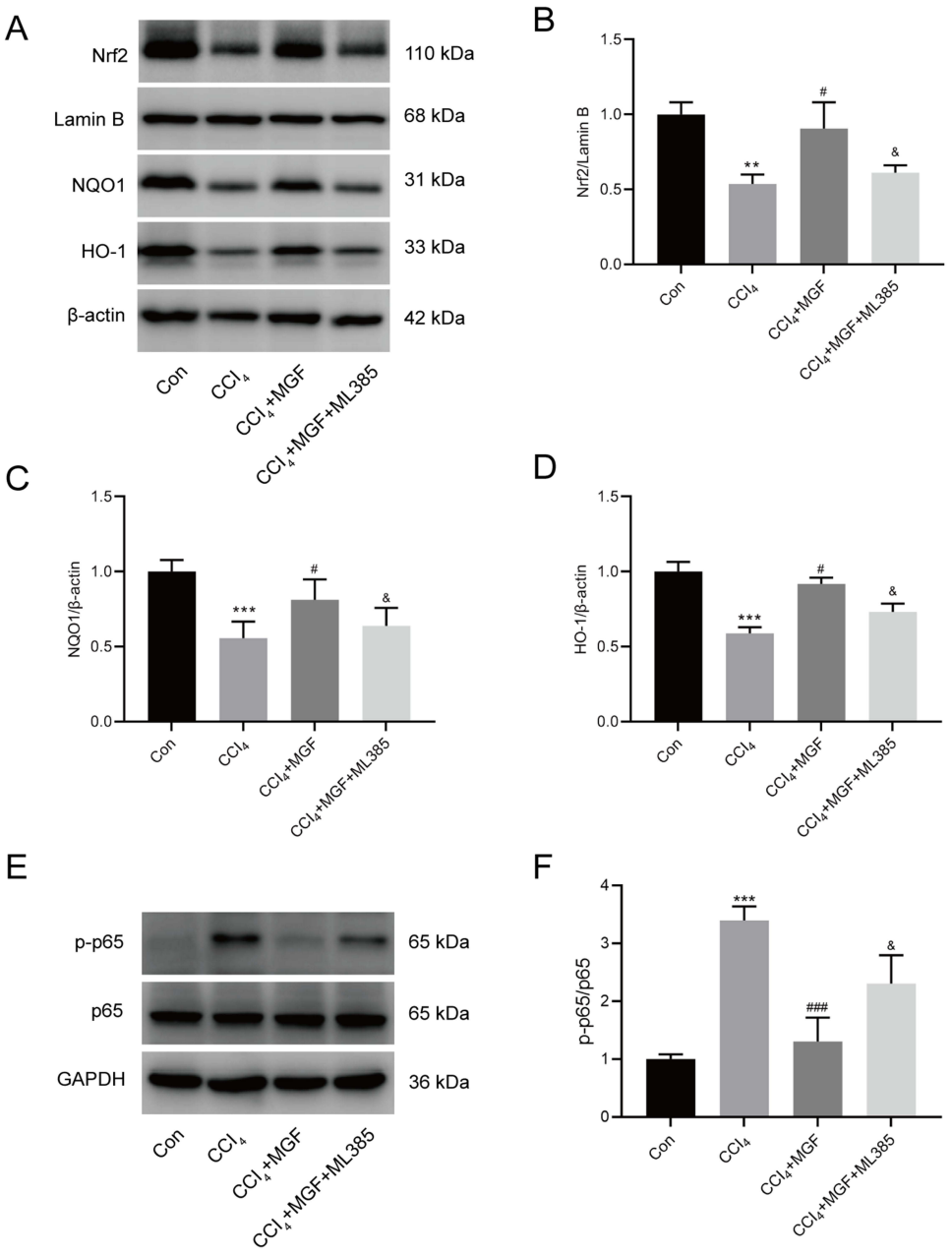

Figure 7 MGF impact on Nrf2 pathway in CCl_4-treated HepG2 cells. (**A**) Indicating Nrf2, NQO1, and HO-1 protein expression in different groups through Western blotting. (**B–D**) Quantifying Western blotting data for Nrf2, NQO1, and HO-1. (**E**) Indicating p-p65 and p65 protein expression in different groups through Western blotting. (**F**) Quantifying Western blotting data for p-p-65/p65. Data are expressed as mean ± SD (n = 6). $^{**}P < 0.01$, $^{***}P < 0.001$ versus control group. $^{\#}P < 0.05$, $^{\#\#\#}P < 0.001$ versus CCl_4 group. $^{\&}P < 0.05$ versus CCl_4+MGF group.

corroborating previous findings.[36] Pretreatment of mice with MGF led to a dose-dependent decrease in ALT and AST levels, thereby substantiating its protective effect against CCl_4-induced ALI.

OS is the primary cause of CCl_4-induced liver injury.[7,37] SOD and GSH are key antioxidants that neutralize ROS and protect cells from damage.[38] MDA, a lipid peroxidation by-product, is an indirect marker of cellular damage.[39] Accordingly, GSH, SOD, and MDA are crucial biomarkers for assessing OS in the liver. It has been demonstrated that CCl_4 exposure results in a reduction in SOD and GSH levels in hepatic tissue, concomitant with an elevation in MDA levels.[30] Furthermore, the administration of antioxidants has been observed to ameliorate liver injury.[40,41] Chowdhury A et al[42] found that MGF could improve the activity of GSH and SOD, and reduce the hepatotoxicity caused by acetaminophen. Our extensive in vivo and in vitro studies consistently demonstrated that treatment with MGF resulted in

increased levels of GSH and SOD, along with a reduction in MDA content in liver tissues and HepG2 cells. These findings suggest that MGF may mitigate liver injury by attenuating oxidative stress.

The complex interaction between inflammation and OS is a critical determinant of CCl_4-induced liver injury.[43] Neutrophils, which serve as key effectors, are robustly activated by CCL_4, releasing inflammatory mediators.[44] Notably, proinflammatory cytokines, such as TNF-α, IL-1β, and IL-6, are instrumental in the pathological progression of ALI, thereby intensifying tissue damage.[45] Excessive free radicals produced during this process exacerbate the inflammatory response by inducing the release of cytokines and activating hepatic macrophages, thereby perpetuating the deleterious cycle of inflammation and OS.[46] Meng X et al[47] reported that CCl_4 can induce the release of TNF-α and IL-1β/6 via the TLR4/NF-κB signaling pathway, thereby initiating hepatic injury. Notably, our findings demonstrated that MGF treatment significantly attenuated the levels of these proinflammatory cytokines in CCl_4-exposed mice and decreased the expression of p-p65, indicating its potential to interrupt the inflammatory cascade and ameliorate liver injury.

The central role of mitochondria as the primary target of CCl_4-mediated apoptosis is well documented.[48] This apoptotic pathway is intricately regulated by anti-apoptotic and pro-apoptotic members of the Bcl-2 family.[49] Specifically, Bcl-2 functions as an anti-apoptotic protein, inhibiting the release of apoptotic effectors such as cytochrome c (cyt-c). In contrast, Bax, a pro-apoptotic protein, antagonizes Bcl-2 to promote the release of cyt-c into the cytoplasm, activating caspase-3 and -9 and initiating apoptosis.[50] Consistent with prior research indicating that CCl_4 induces apoptosis in various tissues and cell types through the mitochondrial pathway,[51] our results demonstrated a marked upregulation of Bax and cleaved Caspase-3 and downregulation of Bcl-2 in mouse livers. These findings further substantiate the role of the mitochondrial apoptotic cascade in mediating CCl_4-induced hepatocellular apoptosis. Remarkably, MGF treatment enhances Bcl-2 expression and reduces Bax and cleaved Caspase-3 levels in mouse liver, indicating its regulatory effect on this pathway. Furthermore, given that mitochondria are the primary targets of ROS attack, with excessive ROS production contributing to OS and mitochondrial dysfunction, our observations indicate that MGF mitigates CCl_4-induced mitochondrial ROS generation and increases ATP levels. Consequently, we hypothesize that MGF directly ameliorates CCl_4-induced excessive hepatocellular apoptosis in mice by alleviating OS.

The Nrf2-ARE pathway constitutes a pivotal endogenous anti-OS mechanism identified to date, acting as a primary means by which cellular systems respond to OS.[52] Under normal conditions, Nrf2 is sequestered in the cytoplasm by interacting with Keap1, a critical regulatory protein. However, in response to OS, Nrf2 translocates to the nucleus, forming heterodimers with Maf proteins and subsequently binding to AREs within the promoters of target genes.[53] This coordinated process initiates the transcription of various antioxidant enzymes, including HO-1, NQO1, and SOD. Previous studies have underscored the vulnerability of the Nrf2 antioxidant defense system to disruption by chemical agents, such as CCl_4, which intensifies hepatic OS.[54] Numerous natural derivatives have exhibited hepatoprotective effects through the activation of the Nrf2 pathway.[55–57] Consistent with these findings, MGF attenuates the activation of the NLRP-3 inflammasome induced by LPS and d-galactosamine while simultaneously activating the Nrf2 pathway.[58] In this study, the proteins Nrf2, NQO1, and HO-1 were significantly downregulated in mouse hepatocytes following CCl_4-induced injury, a finding that aligns with previous research.[48] Conversely, administration of MGF led to a marked upregulation of these proteins, suggesting that MGF may mitigate CCl_4-induced ALI by activating the Nrf2-ARE pathway. This hypothesis is further substantiated by in vitro studies, which illustrate that MGF mitigates CCl_4-induced hepatocyte damage through Nrf2 pathway activation. Conversely, the administration of ML385, an inhibitor of Nrf2 activation, nullifies this protective effect. Due to practical constraints, we could not determine the impact of MGF on liver injury in $Nrf2^{-/-}$ mice within the scope of this research. Additionally, our findings do not definitively exclude the possibility that MGF may mitigate ALI through mechanisms independent of the Nrf2 signaling pathway.

Conclusions

Our findings indicate that CCl_4 can induce liver injury, whereas treatment with MGF mitigates ALI by inhibiting OS, inflammation, and apoptosis (Figure 8). The protective mechanism of MGF is mediated by the Nrf2-ARE pathway activation.

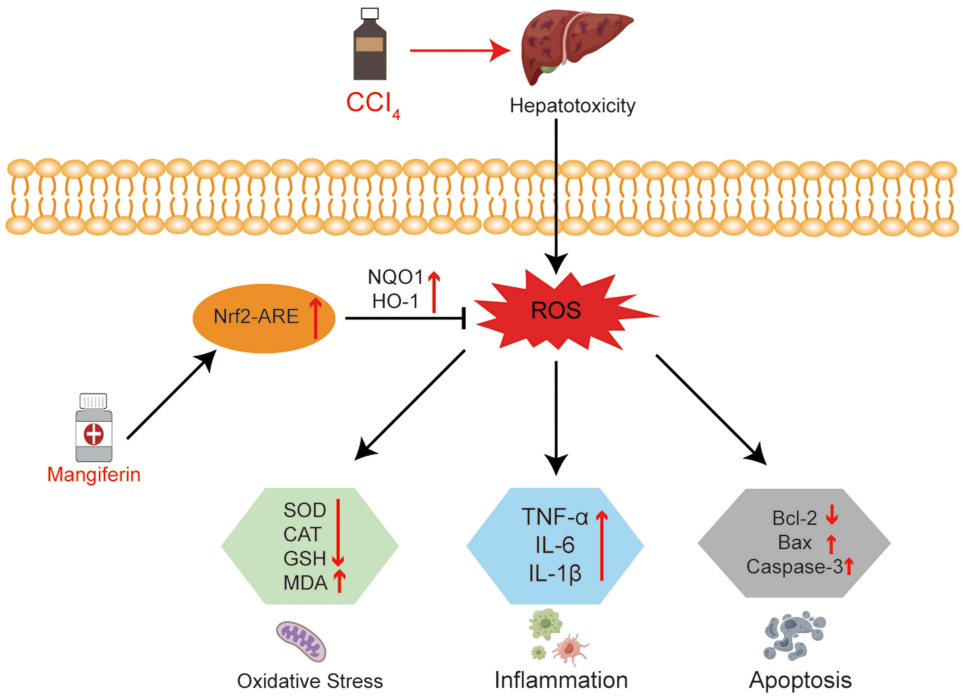

Figure 8 Mechanism of MGF protective impact against hepatotoxicity induced by CCl_4.

Acknowledgments

We appreciate Dr. Chunyu Bai and Dr. Jing Yan for helping with language editing and figure artwork.

Funding

Funded by Projects of Medical and Health Technology Development Program in Shandong Province, China (No. 202202040316), the Research Fund for Lin He's Academician Workstation of New Medicine and Clinical Translation in Jining Medical University (No. JYHL2022MS19), and Training Program of Innovation and Entrepreneurship for Undergraduates in Jining Medical University (No. cx2023193).

Disclosure

The authors report no conflicts of interest in this work.

References

1. Trefts E, Gannon M, Wasserman DH. The liver. *Curr Biol*. 2017;27(21):R1147–r1151. doi:10.1016/j.cub.2017.09.019
2. Tak J, Kim YS, Kim TH, Park GC, Hwang S, Kim SG. Galpha(12) overexpression in hepatocytes by ER stress exacerbates acute liver injury via ROCK1-mediated miR-15a and ALOX12 dysregulation. *Theranostics*. 2022;12(4):1570–1588. doi:10.7150/thno.67722
3. Bakhshi A, Eslami N, Norouzi N, Letafatkar N, Amini-Salehi E, Hassanipour S. The association between various viral infections and multiple sclerosis: an umbrella review on systematic review and meta-analysis. *Rev Med Virol*. 2024;34(1):e2494. doi:10.1002/rmv.2494
4. Wang Z, Zhu S, Jia Y, et al. Positive selection of somatically mutated clones identifies adaptive pathways in metabolic liver disease. *Cell*. 2023;186(9):1968–1984e20. doi:10.1016/j.cell.2023.03.014
5. Yang S, Kuang G, Zhang L, et al. Mangiferin attenuates LPS/D-galn-induced acute liver injury by promoting HO-1 in Kupffer cells. *Front Immunol*. 2020;11:285. doi:10.3389/fimmu.2020.00285
6. Czekaj P, Krol M, Kolanko E, et al. Dynamics of chronic liver injury in experimental models of hepatotoxicity. *Front Biosci*. 2023;28(5):87. doi:10.31083/j.fbl2805087
7. Rahmani AH, Almatroudi A, Allemailem KS, et al. Oleuropein, a phenolic component of Olea europaea L. ameliorates CCl4-induced liver injury in rats through the regulation of oxidative stress and inflammation. *Eur Rev Med Pharmacol Sci*. 2024;28(4):1259–1271. doi:10.26355/eurrev_202402_35447
8. Zhang X, Kuang G, Wan J, et al. Salidroside protects mice against CCl4-induced acute liver injury via down-regulating CYP2E1 expression and inhibiting NLRP3 inflammasome activation. *Int Immunopharmacol*. 2020;85:106662. doi:10.1016/j.intimp.2020.106662

9. Unsal V, Cicek M, Sabancilar I. Toxicity of carbon tetrachloride, free radicals and role of antioxidants. *Rev Environ Health*. 2021;36(2):279–295. doi:10.1515/reveh-2020-0048
10. Wang T, Zhang J, Wei H, et al. Matrine-induced nephrotoxicity via GSK-3beta/nrf2-mediated mitochondria-dependent apoptosis. *Chem Biol Interact*. 2023;378:110492. doi:10.1016/j.cbi.2023.110492
11. Canning P, Sorrell FJ, Bullock AN. Structural basis of Keap1 interactions with Nrf2. *Free Radic Biol Med*. 2015;88(Pt B):101–107. doi:10.1016/j.freeradbiomed.2015.05.034
12. Hu R, Wu F, Zheng YQ. Ivacaftor attenuates gentamicin-induced ototoxicity through the CFTR-Nrf2-HO1/NQO1 pathway. *Redox Rep*. 2024;29(1):2332038. doi:10.1080/13510002.2024.2332038
13. Gao Z, Yi W, Tang J, et al. Urolithin A protects against Acetaminophen-induced liver injury in mice via sustained activation of Nrf2. *Int J Biol Sci*. 2022;18(5):2146–2162. doi:10.7150/ijbs.69116
14. Chen L, Li S, Zhu J, et al. Mangiferin prevents myocardial infarction-induced apoptosis and heart failure in mice by activating the Sirt1/FoxO3a pathway. *J Cell Mol Med*. 2021;25(6):2944–2955. doi:10.1111/jcmm.16329
15. Wang Y, Guo X, Fan X, Zhang H, Xue D, Pan Z. The protective effect of mangiferin on osteoarthritis: an in vitro and in vivo study. *Physiol Res*. 2022;71(1):135–145. doi:10.33549/physiolres.934747
16. Ito T, Kakino M, Tazawa S, et al. Quantification of polyphenols and pharmacological analysis of water and ethanol-based extracts of cultivated agarwood leaves. *J Nutr Sci Vitaminol*. 2012;58(2):136–142. doi:10.3177/jnsv.58.136
17. Suliman RS, Ali HS, Alhelal K, et al. Antioxidant properties of Solenostemma argel effervescent tablets. *Curr Pharm Biotechnol*. 2019;20(8):679–688. doi:10.2174/1389201020666190617165300
18. Mei S, Ma H, Chen X. Anticancer and anti-inflammatory properties of mangiferin: a review of its molecular mechanisms. *Food Chem Toxicol*. 2021;149:111997. doi:10.1016/j.fct.2021.111997
19. Lebaka VR, Wee YJ, Ye W, Korivi M. nutritional composition and bioactive compounds in three different parts of mango fruit. *Int J Environ Res Public Health*. 2021;18(2):741. doi:10.3390/ijerph18020741
20. Li N, Xiong R, He R, Liu B, Wang B, Geng Q. Mangiferin mitigates lipopolysaccharide-induced lung injury by inhibiting NLRP3 inflammasome activation. *J Inflamm Res*. 2021;14:2289–2300. doi:10.2147/JIR.S304492
21. Sahu AK, Verma VK, Mutneja E, et al. Mangiferin attenuates cisplatin-induced acute kidney injury in rats mediating modulation of MAPK pathway. *Mol Cell Biochem*. 2019;452(1–2):141–152. doi:10.1007/s11010-018-3420-y
22. Song J, Meng Y, Wang M, et al. Mangiferin activates Nrf2 to attenuate cardiac fibrosis via redistributing glutaminolysis-derived glutamate. *Pharmacol Res*. 2020;157:104845. doi:10.1016/j.phrs.2020.104845
23. Saviano A, Raucci F, Casillo GM, et al. Anti-inflammatory and immunomodulatory activity of Mangifera indica L. reveals the modulation of COX-2/mPGES-1 axis and Th17/Treg ratio. *Pharmacol Res*. 2022;182:106283. doi:10.1016/j.phrs.2022.106283
24. Wang M, Zhang Z, Huo Q, et al. targeted polymeric nanoparticles based on mangiferin for enhanced protection of pancreatic beta-cells and type 1 diabetes mellitus efficacy. *ACS Appl Mater Interfaces*. 2022;14(9):11092–11103. doi:10.1021/acsami.1c22964
25. Hou S, Wang F, Li Y, et al. Pharmacokinetic study of mangiferin in human plasma after oral administration. *Food Chem*. 2012;132(1):289–294. doi:10.1016/j.foodchem.2011.10.079
26. Ismail MB, Rajendran P, AbuZahra HM, Veeraraghavan VP. Mangiferin inhibits apoptosis in doxorubicin-induced vascular endothelial cells via the nrf2 signaling pathway. *Int J Mol Sci*. 2021;22(8):4259. doi:10.3390/ijms22084259
27. Xia G, Li X, Zhu X, Yin X, Ding H, Qiao Y. Mangiferin protects osteoblast against oxidative damage by modulation of ERK5/Nrf2 signaling. *Biochem Biophys Res Commun*. 2017;491(3):807–813. doi:10.1016/j.bbrc.2017.06.184
28. Li L, Lan Y, Wang F, Gao T. Linarin protects against CCl(4)-induced acute liver injury via activating autophagy and inhibiting the inflammatory response: involving the TLR4/MAPK/Nrf2 pathway. *Drug Des Devel Ther*. 2023;17:3589–3604. doi:10.2147/DDDT.S433591
29. Ge PX, Tai T, Jiang LP, et al. Choline and trimethylamine N-oxide impair metabolic activation of and platelet response to clopidogrel through activation of the NOX/ROS/Nrf2/CES1 pathway. *J Thromb Haemost*. 2023;21(1):117–132. doi:10.1016/j.jtha.2022.10.010
30. Li Q, Zhang W, Cheng N, et al. Pectolinarigenin ameliorates Acetaminophen-induced acute liver injury via attenuating oxidative stress and inflammatory response in Nrf2 and PPARa dependent manners. *Phytomedicine*. 2023;113:154726. doi:10.1016/j.phymed.2023.154726
31. Wong RJ, Kachru N, Martinez DJ, Moynihan M, Ozbay AB, Gordon SC. real-world comorbidity burden, health care utilization, and costs of nonalcoholic steatohepatitis patients with advanced liver diseases. *J Clin Gastroenterol*. 2021;55(10):891–902. doi:10.1097/MCG.0000000000001409
32. Datta S, Aggarwal D, Sehrawat N, et al. Hepatoprotective effects of natural drugs: current trends, scope, relevance and future perspectives. *Phytomedicine*. 2023;121:155100. doi:10.1016/j.phymed.2023.155100
33. Wang A, Li M, Huang H, et al. A review of Penthorum chinense Pursh for hepatoprotection: traditional use, phytochemistry, pharmacology, toxicology and clinical trials. *J Ethnopharmacol*. 2020;251:112569. doi:10.1016/j.jep.2020.112569
34. Yuan R, Tao X, Liang S, et al. Protective effect of acidic polysaccharide from Schisandra chinensis on acute ethanol-induced liver injury through reducing CYP2E1-dependent oxidative stress. *Biomed Pharmacother*. 2018;99:537–542. doi:10.1016/j.biopha.2018.01.079
35. Chinnappan R, Mir TA, Alsalameh S, et al. low-cost point-of-care monitoring of alt and ast is promising for faster decision making and diagnosis of acute liver injury. *Diagnostics*. 2023;13(18). doi:10.3390/diagnostics13182967
36. Cao Z, Lu P, Li L, et al. Bioinformatics-led discovery of liver-specific genes and macrophage infiltration in acute liver injury. *Front Immunol*. 2023;14:1287136. doi:10.3389/fimmu.2023.1287136
37. Gong Q, Wang X, Liu Y, et al. Potential hepatoprotective effects of allicin on carbon tetrachloride-induced acute liver injury in mice by inhibiting oxidative stress, inflammation, and apoptosis. *Toxics*. 2024;12(5):328. doi:10.3390/toxics12050328
38. Lee B, Afshari NA, Shaw PX. Oxidative stress and antioxidants in cataract development. *Curr Opin Ophthalmol*. 2024;35(1):57–63. doi:10.1097/ICU.0000000000001009
39. Zhao Y, Zhou C, Guo X, et al. Exposed to mercury-induced oxidative stress, changes of intestinal microflora, and association between them in mice. *Biol Trace Elem Res*. 2021;199(5):1900–1907. doi:10.1007/s12011-020-02300-x
40. Awny MM, Al-Mokaddem AK, Ali BM. Mangiferin mitigates di-(2-ethylhexyl) phthalate-induced testicular injury in rats by modulating oxidative stress-mediated signals, inflammatory cascades, apoptotic pathways, and steroidogenesis. *Arch Biochem Biophys*. 2021;711:108982. doi:10.1016/j.abb.2021.108982

41. Cai X, Cai H, Wang J, et al. Molecular pathogenesis of Acetaminophen-induced liver injury and its treatment options. *J Zhejiang Univ Sci B*. 2022;23(4):265–285. doi:10.1631/jzus.B2100977
42. Chowdhury A, Lu J, Zhang R, et al. Mangiferin ameliorates Acetaminophen-induced hepatotoxicity through APAP-Cys and JNK modulation. *Biomed Pharmacother*. 2019;117:109097. doi:10.1016/j.biopha.2019.109097
43. Wu S, Wen F, Zhong X, Du W, Chen M, Wang J. Astragaloside IV ameliorate acute alcohol-induced liver injury in mice via modulating gut microbiota and regulating NLRP3/caspase-1 signaling pathway. *Ann Med*. 2023;55(1):2216942. doi:10.1080/07853890.2023.2216942
44. Zhou J, Li J, Yu Y, et al. Mannan-binding lectin deficiency exacerbates sterile liver injury in mice through enhancing hepatic neutrophil recruitment. *J Leukoc Biol*. 2019;105(1):177–186. doi:10.1002/JLB.3A0718-251R
45. Li SL, Wang ZM, Xu C, et al. Liraglutide attenuates hepatic ischemia-reperfusion injury by modulating macrophage polarization. *Front Immunol*. 2022;13:869050. doi:10.3389/fimmu.2022.869050
46. Singh V, Ubaid S. Role of Silent Information Regulator 1 (SIRT1) in regulating oxidative stress and inflammation. *Inflammation*. 2020;43(5):1589–1598. doi:10.1007/s10753-020-01242-9
47. Meng X, Kuang H, Wang Q, Zhang H, Wang D, Kang T. A polysaccharide from Codonopsis pilosula roots attenuates carbon tetrachloride-induced liver fibrosis via modulation of TLR4/NF-kappaB and TGF-beta1/Smad3 signaling pathway. *Int Immunopharmacol*. 2023;119:110180. doi:10.1016/j.intimp.2023.110180
48. Bi Y, Liu S, Qin X, et al. FUNDC1 interacts with GPx4 to govern hepatic ferroptosis and fibrotic injury through a mitophagy-dependent manner. *J Adv Res*. 2024;55:45–60. doi:10.1016/j.jare.2023.02.012
49. Iksen, Witayateeraporn W, Hardianti B, Pongrakhananon V, Pongrakhananon V. Comprehensive review of Bcl-2 family proteins in cancer apoptosis: therapeutic strategies and promising updates of natural bioactive compounds and small molecules. *Phytother Res*. 2024;38(5):2249–2275. doi:10.1002/ptr.8157
50. Li Z, Zhang R, Yin X, et al. Realgar (As(4)S(4)), a traditional Chinese medicine, induces acute promyelocytic leukemia cell death via the Bcl-2/Bax/Cyt-C/AIF signaling pathway in vitro. *Aging*. 2022;14(17):7109–7125. doi:10.18632/aging.204281
51. Yu Z, Li Q, Wang Y, Li P. A potent protective effect of baicalein on liver injury by regulating mitochondria-related apoptosis. *Apoptosis*. 2020;25(5–6):412–425. doi:10.1007/s10495-020-01608-2
52. Liu S, Pi J, Zhang Q. Signal amplification in the KEAP1-NRF2-ARE antioxidant response pathway. *Redox Biol*. 2022;54:102389. doi:10.1016/j.redox.2022.102389
53. Adelusi TI, Du L, Hao M, et al. Keap1/Nrf2/ARE signaling unfolds therapeutic targets for redox imbalanced-mediated diseases and diabetic nephropathy. *Biomed Pharmacother*. 2020;123:109732. doi:10.1016/j.biopha.2019.109732
54. Li X, Wang J, Li Y, et al. The gp130/STAT3-endoplasmic reticulum stress axis regulates hepatocyte necroptosis in acute liver injury. *Croat Med J*. 2023;64(3):149–163. doi:10.3325/cmj.2023.64.149
55. Li H, Weng Q, Gong S, et al. Kaempferol prevents Acetaminophen-induced liver injury by suppressing hepatocyte ferroptosis via Nrf2 pathway activation. *Food Funct*. 2023;14(4):1884–1896. doi:10.1039/d2fo02716j
56. Hong MK, Hu LL, Zhang YX, et al. 6-Gingerol ameliorates sepsis-induced liver injury through the Nrf2 pathway. *Int Immunopharmacol*. 2020;80:106196. doi:10.1016/j.intimp.2020.106196
57. Liu L, Zhang X, Xing X, et al. Triptolide induces liver injury by regulating macrophage recruitment and polarization via the Nrf2 signaling pathway. *Oxid Med Cell Longev*. 2022;2022:1492239. doi:10.1155/2022/1492239
58. Pan CW, Pan ZZ, Hu JJ, et al. Mangiferin alleviates lipopolysaccharide and D-galactosamine-induced acute liver injury by activating the Nrf2 pathway and inhibiting NLRP3 inflammasome activation. *Eur J Pharmacol*. 2016;770:85–91. doi:10.1016/j.ejphar.2015.12.006